ACS Photonics

pubs.acs.org/journal/apchd5

Article

Giant Intrinsic Chirality in Curled Metasurfaces

Chao Wang,[‡] Zhancheng Li,[‡] Ruhao Pan, Wenwei Liu, Hua Cheng,* Junjie Li, Wenyuan Zhou, Jianguo Tian, and Shuqi Chen*

Cite This: *ACS Photonics* 2020, 7, 3415−3422

Read Online

ACCESS | Metrics & More | Article Recommendations | Supporting Information

ABSTRACT: Artificial nanostructures, whose spatial symmetry can be arbitrarily designed, play an ever more critical role for the realization of giant chiral optical responses. In order to break the mirror symmetry of the whole structure to realize a chiral optical response, there-dimensional geometries or multilayers of nanostructures were involved in the previous designs of chiral nanostructures, which may not be appealing from an application perspective due to their complexities and fabrication challenges. Here, we theoretically and experimentally demonstrate the use of curled metasurfaces for the implementation of giant intrinsic chiral optical responses in the near-infrared regime. Different from previous approaches, the giant chiral optical responses in the proposed curled metasurfaces are mainly attributed to the breaking of the mirror symmetry of the whole structure by involving curled nanostructures standing along horizontal rectangular apertures. Spin-selective transmission with over 60% efficiency has been experimentally proved with L-shaped curled metasurfaces. The proposed curled metasurfaces provide a new strategy for the realization of giant intrinsic chirality, which shows a great potential for practical application in spin optics and chiral sensing.

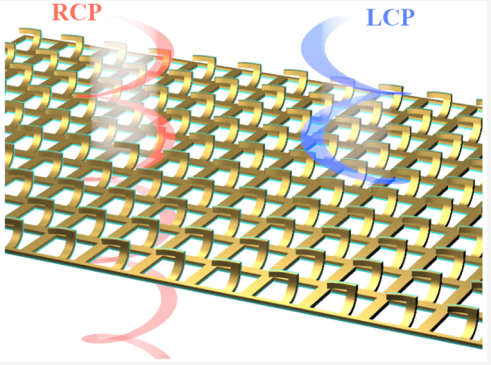

KEYWORDS: *curled metasurfaces, intrinsic chirality, chiral optical response, spin-selective transmission, high efficiency*

Chirality, omnipresent in our daily life, is a common feature of object whose structure cannot be superimposed upon its own mirror image.[1,2] Chirality plays a key role in some biochemical processes, so the study and discrimination of chirality have received significant attention of scientific community. Nowadays, the discrimination of chirality is always associated with the interaction between the chiral objects and the helicity optical waves.[3] Circular dichroism (CD) spectrum, which is defined as the difference in absorption for optical waves with opposite helicities, is the main approach for chirality detection and discrimination. However, ascribing to the fundamental mismatch in size scale between molecules and the wavelength of optical waves, the CD signals of nature chiral materials are extremely weak, which prevents the study and application of chirality.

Recently, the development of metamaterials and metasurfaces provides an alternative approach for the realization of giant chiral optical responses.[3−7] They are artificial periodic arrays with subwavelength unit structures whose spatial symmetry can be arbitrarily designed.[8] By utilizing different unit structures to break the mirror symmetry of the whole structure, they have been widely proposed to realize the significant enhancement of the chiral optical response.[9−15] In the past several years, not only the three-dimensional (3D) chirality (intrinsic chirality), but also the planar chirality and the extrinsic chirality in metamaterials and metasurfaces have been widely investigated.[16−21] The nanostructures with different chiral optical responses have been extensively applied in spin optics, such as chiral meta-hologram, circularly polarized light detection, chiral mirrors, nonlinear chiral response, and so on.[22−26] The latest breakthroughs further validated that chiral nanostructures with spin-controlled wavefront shaping functionalities can find more applications in multifunctional polarizers, optical encryption and decryption, chiral imaging, and optical information processing.[27−29] Specially, the artificial nanostructures with giant chiral optical responses have emerged as a powerful platform for biosensing, which allow not only the unambiguous detection of large chiral molecules, but also the discrimination of the chiral molecules down to zeptomole levels.[30−34]

For the realization of giant intrinsic chirality, complex 3D geometries or multilayers of nanostructures are always utilized to break the mirror symmetry of the whole structure.[35−38] However, these designs, based on traditional fabrication processes with multilayer stacking of two-dimensional (2D) pattern or direct writing technologies, may not be appealing

Received: August 4, 2020
Published: December 4, 2020

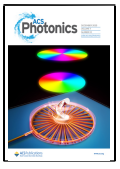

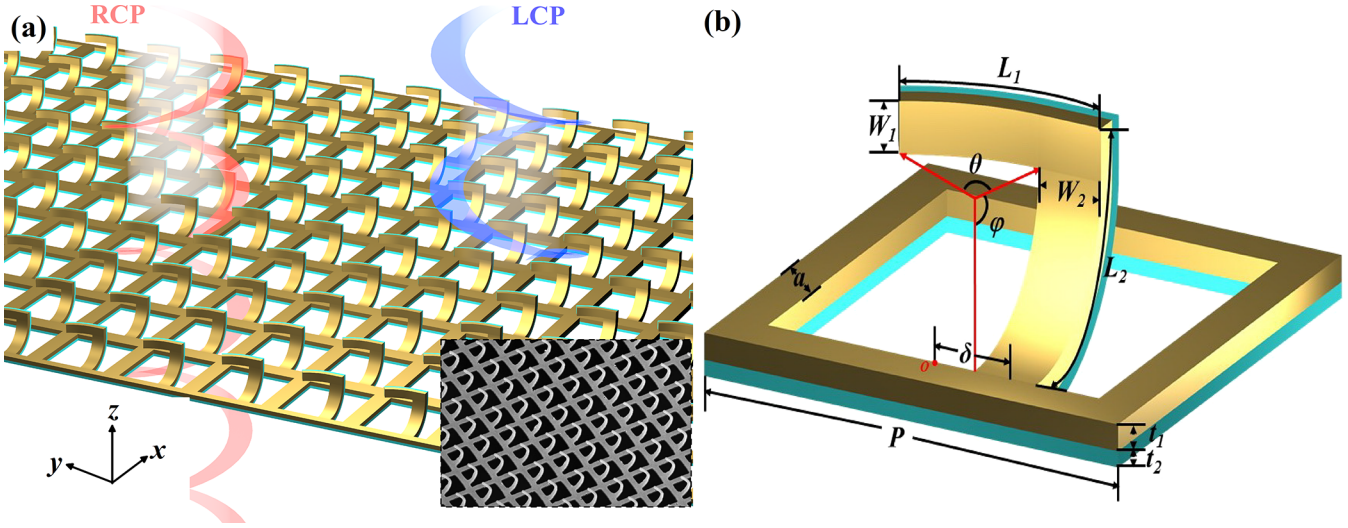

Figure 1. (a) Schematic of a designed L-shaped curled metasurface, which shows a left-handed chirality. Inset: Scanning electron microscope (SEM) image of the fabricated metasurface. (b) Structural parameters of a unit cell.

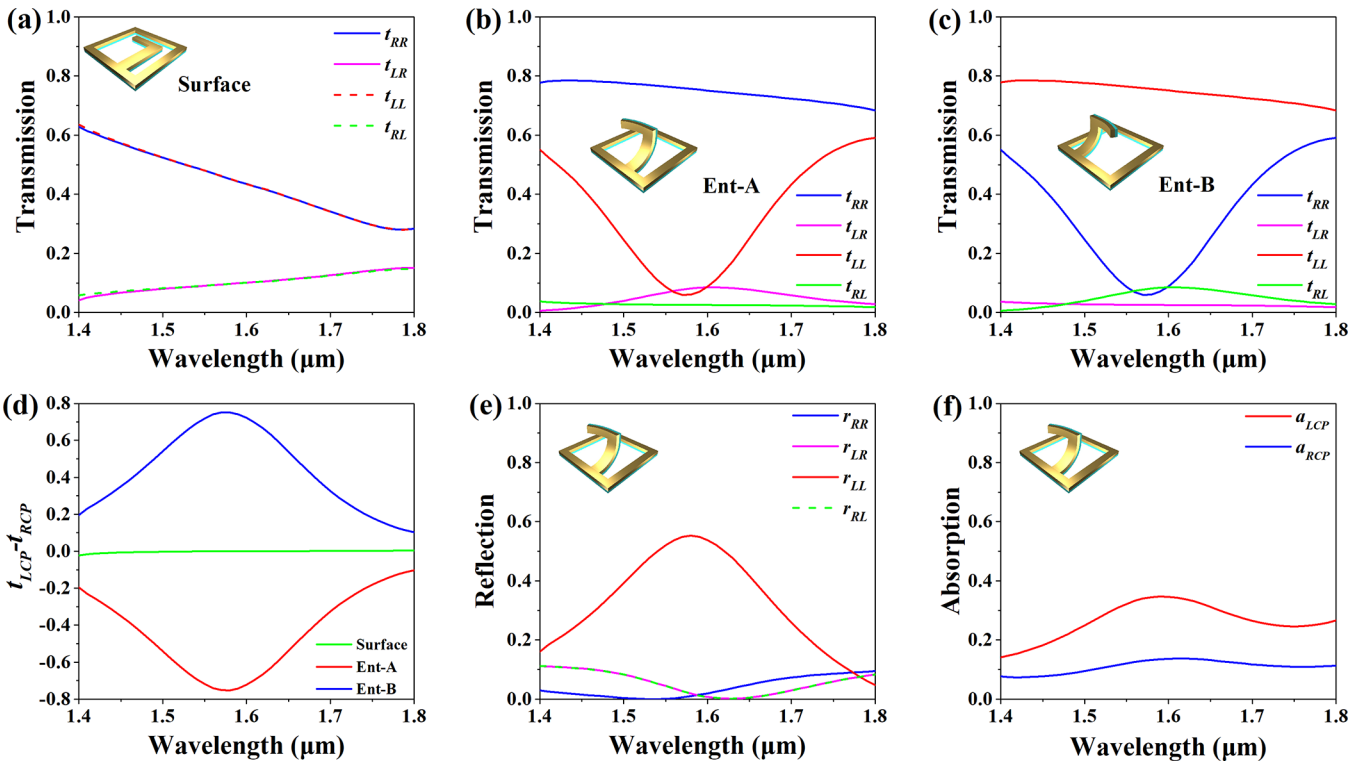

Figure 2. Squared moduli of **T** matrix coefficients of the designed curled metasurfaces. The orientation and curl angles ϕ and θ of the L-shaped resonators are different: (a) Left orientation with curl angles ϕ and θ equal to zero. (b) Left orientation with curl angles ϕ and θ equals to 90° and 51.5°. (c) Right orientation with curl angles ϕ and θ equals to 90° and 51.5°. (d) The difference of the transmission intensity $\Delta t = t_{LCP} - t_{RCP}$ for three designed metasurfaces in (a)−(c). Simulated results of the (e) reflection spectra and (f) absorption spectra for the Ent-A under LCP and RCP illuminations.

from an application perspective due to their complexities and fabrication challenges. Through some exquisite structural designs, the recent advances in dielectric chiral metasurfaces have proved their abilities to achieve giant chiral optical response. These designs composed of monolayer or bilayer nanostructures can effectively reduce the complexity of fabrication, which emerge as a good platform for the realization of giant intrinsic chiral optical responses.[16,21] On the other hand, we proposed a focused ion beam (FIB) induced folding technique to construct 3D geometries based on planar suspended nanostructures, which provides a new alternative method for the breaking of the structural mirror symmetry of metasurfaces and show endless possibilities for the implementation of nanostructures with intrinsic chirality.[39−41] Nevertheless, this technique has a slow fabrication speed and a low spatial controllability, resulting in time-consuming fabrication process and structural geometry size in micron scale. A simple approach for the realization of giant intrinsic chiral optical

https://dx.doi.org/10.1021/acsphotonics.0c01230
ACS Photonics 2020, 7, 3415−3422

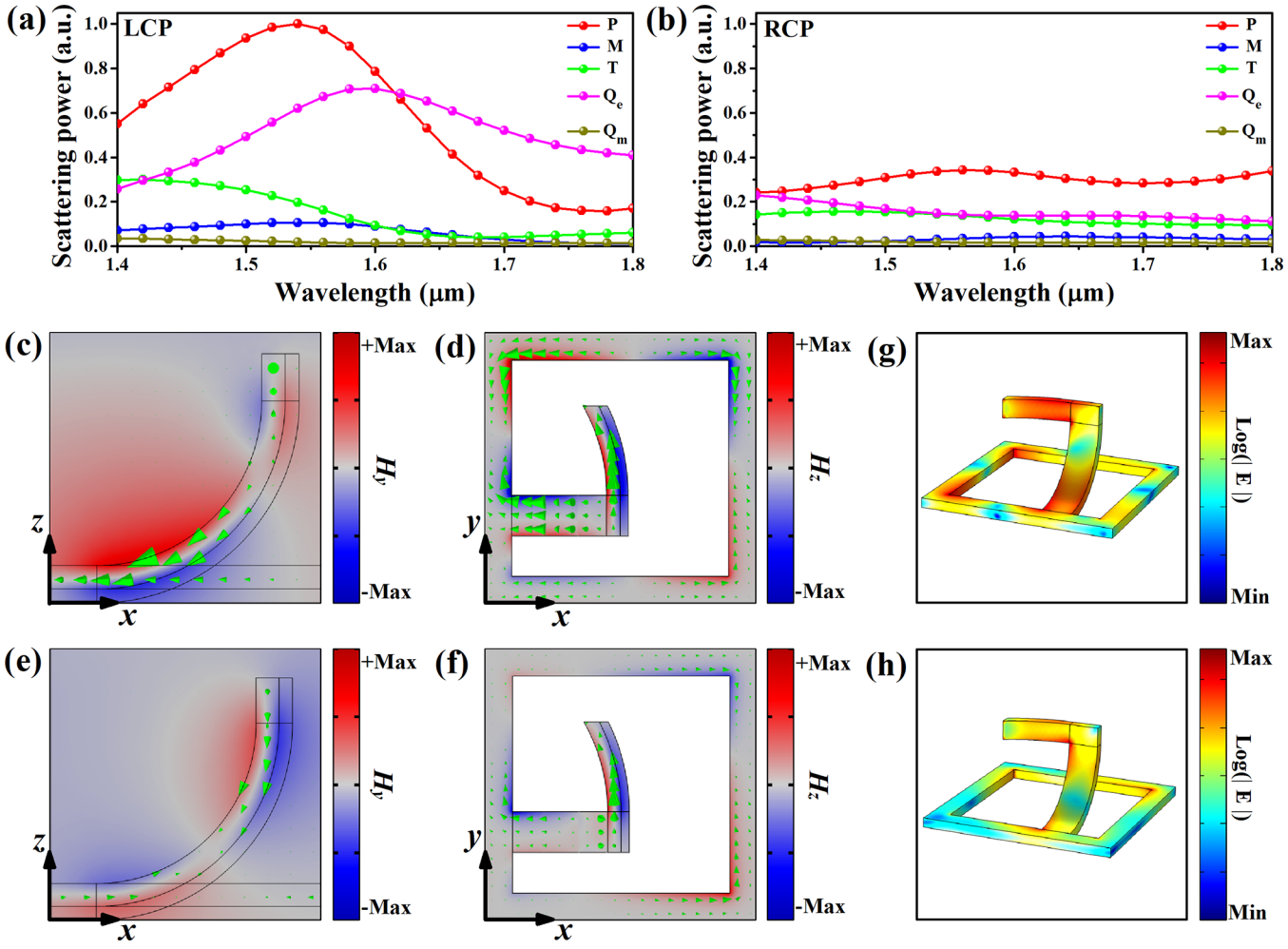

Figure 3. Multipolar decomposition of the scattering spectra for the Ent-A in terms of electric dipole (P), magnetic dipole (M), toroidal dipole (T), electric quadrupole (Q_e), and magnetic quadrupole (Q_m) under (a) LCP and (b) RCP illuminations. The current flow (green arrows) in the Ent-A ((c, e) on the middle section of the upright rod and (d, f) in the whole structure) and the corresponding distribution of the *y*- and *z*-component of the magnetic field at the wavelength of 1.58 μm under (c, d) LCP and (e, f) RCP illuminations. Simulated electric field distributions on the surface of the Ent-A under (g) LCP and (h) RCP illuminations at the wavelength of 1.58 μm.

response in the visible and near-infrared regime is still highly desirable.

Here, we theoretically and experimentally demonstrate that the proposed curled metasurfaces can realize the giant intrinsic chiral optical response in the near-infrared regime, which can be easily fabricated by FIB-induced bending technology. The giant chiral optical response is mainly attributed to the breaking of the mirror symmetry of the whole structure by involving the curled nanostructures standing along horizontal rectangular apertures. Two L-shaped curled metasurfaces with opposite chiral optical responses are proposed to realize the spin-selective transmission of optical waves, which have over 60% experimentally measured efficiency. To further reveal the broader possibilities of the curled metasurfaces for the implementation of giant chiral optical responses, a T-shaped curled metasurface with opposite chiral optical responses at two adjacent wavebands is also theoretically and experimentally validated. The proposed curled metasurfaces provide a good alternative strategy for the realization of giant intrinsic chiral optical response, which shows a great potential for practical applications in spin optics and chiral sensing.

Figure 1a is a schematic showing the chiral optical response of a curled metasurface that we designed, which is composed of L-shaped curled nanostructures and horizontal rectangular apertures. The proposed L-shaped curled metasurface can transmit right-handed circular polarized (RCP) wave without polarization change while preventing the transmission of left-handed circular polarized (LCP) wave. Both the L-shaped curled nanostructures and the horizontal rectangular apertures consist of two layers: a gold layer is attached on a SiN_x layer. The structural parameters of a unit cell are shown in Figure 1b, where the periods P in both the x- and y-directions are equal to 1 μm. The dimensions of the L-shaped curled nanostructures are L_1 = 494 nm, W_1 = 100 nm, L_2 = 650 nm, and W_2 = 150 nm. The thicknesses of the gold layer t_1 and the SiN_x layer t_2 are 50 and 30 nm, respectively. The distance between the upright rod and the central axis is δ = 175 nm and the width of the horizontal rectangular apertures is a = 100 nm. The curled angle ϕ and θ equal to 90° and 51.5°, respectively.

To make a quantitative analysis on the chiral optical responses of the designed curled metasurfaces, we simulated and compared the coefficients of **T** matrix (for circularly polarized light) of the designed planar and curled metasurfaces. Figure 2 shows the calculated modular square $t_{ij} = |T_{ij}|^2$ (the subscripts "*i*" and "*j*" indicate the polarization state of transmitted and incident optical waves, respectively) of

https://dx.doi.org/10.1021/acsphotonics.0c01230
ACS Photonics 2020, 7, 3415−3422

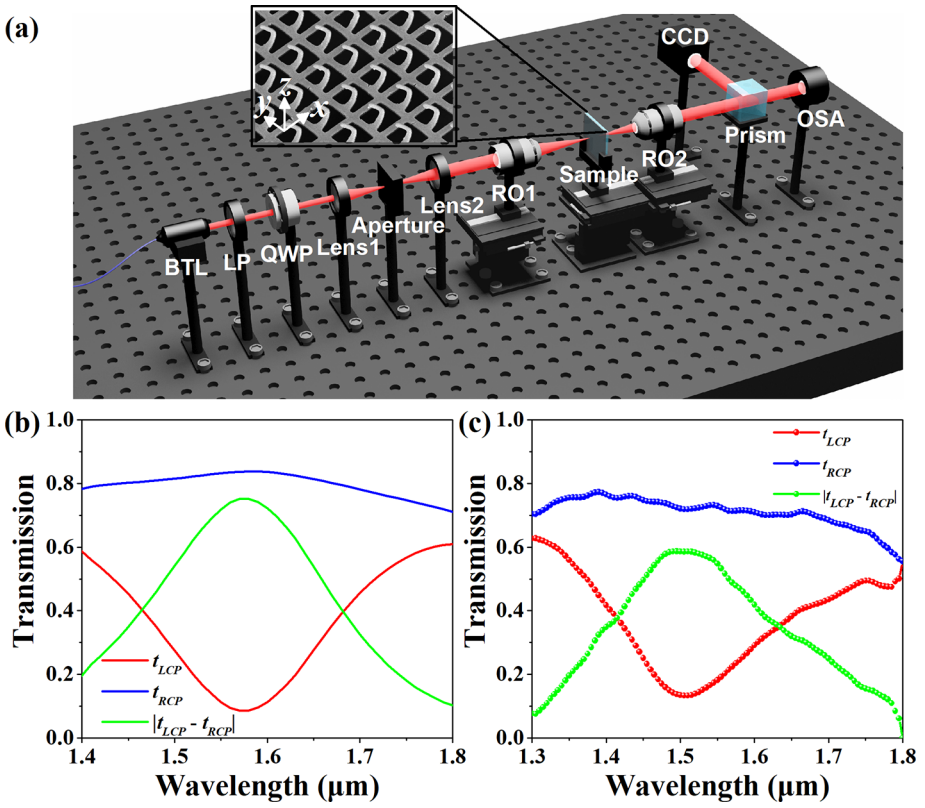

Figure 4. (a) Illustration of the setup for the measurement of chirality in the curled metasurface: BTL, bromine tungsten lamp; LP, linear polarizer; QWP, quarter-wave plate; RO, reflective objective; OSA, optical spectrum analyzer. (b) Simulated and (c) measured transmission spectra and the absolute value of the transmission difference for the Ent-A under LCP and RCP illuminations.

transmission coefficients of the L-shaped planar and curled metasurfaces. The L-shaped planar metasurface does not show any intrinsic chiral optical response in the broad bandwidth since the whole structure is mirror symmetric with respect to the plane parallel to its surface without considering the influence of substrate, as shown in Figure 2a. To the contrary, the L-shaped curled nanostructures can show significant chiral optical response in the whole bandwidth. As shown in Figure 2b,c, the L-shaped curled metasurfaces with opposite orientation directions can exhibit opposite intrinsic chiral optical responses with limited polarization conversion effect (t_{LR} and t_{RL} are very small). Specifically, the efficiency of the spin-selective transmission can reach over 75% at the wavelength of 1.58 μm. The L-shaped curled metasurface with left orientation (Ent-A) can transmit RCP wave without polarization change while preventing the transmission of LCP wave. For the L-shaped curled metasurface with right orientation (Ent-B), the situation is opposite. To further characterize the chiral optical responses of the designed curled metasurfaces, we calculated the difference of the transmission intensity Δt between LCP and RCP incidences, as shown in Figure 2d. The calculated results visually reflect the opposite chiral optical responses of the Ent-A and Ent-B, while the Δt in both designs are over 75%. We further analyzed the variation of the chiral optical response of the Ent-A at various incident angles (Supporting Information, Figure S1), and the results indicate that Δt keeps over 50% when the incident angle is below 10°. The spin-selective transmission in the L-shaped curled metasurface is mainly attributed to the spin-selective interaction between the L-shaped curled metasurface and the LCP (or RCP) wave. According to the reflection and absorption spectra shown in Figure 2e,f, the interaction between the Ent-A and the LCP wave is much stronger, resulting in the enhanced absorption and reflection while the reflection plays a dominate role.

To more specifically and quantitatively elucidate the physical mechanisms, we utilized the electromagnetic multipole expansion method to calculate the power scattered by individual multipoles in the Ent-A under LCP and RCP illuminations.[42] As shown in Figure 3a,b, the scattering power of individual multipoles in the Ent-A under LCP illumination is much bigger than that under RCP illumination. This validates that the interaction between the Ent-A and LCP illumination is much stronger, resulting in the decreasing of the transmission intensity. The results also validate that the spin-selective excitations of the electric dipole and the electric quadrupole dominate the chiral optical response of the Ent-A, which is in good agreement with the simulated results of the current flow and the magnetic field distribution within the nanostructure (Figure 3c–f). A strong current flow along the upright curled rod can be observed under LCP illumination at the wavelength of 1.58 μm, which is related to the excitation of an electric dipole along the x-direction. The electric quadrupole in the x–y plane is excited by the current flow within the horizontal rectangular aperture. The current flow in the Ent-A under RCP illumination is mainly within the horizontal rod, which is related to the excitation of an electric dipole along the y-direction. The quantitative analysis of the components of the excited electric dipole and electric quadrupole under both LCP and RCP illuminations can be found in the Supporting Information, Figure S2. Apparently, the interaction between the Ent-A and RCP wave is relatively weak, which can be

https://dx.doi.org/10.1021/acsphotonics.0c01230
ACS Photonics 2020, 7, 3415–3422

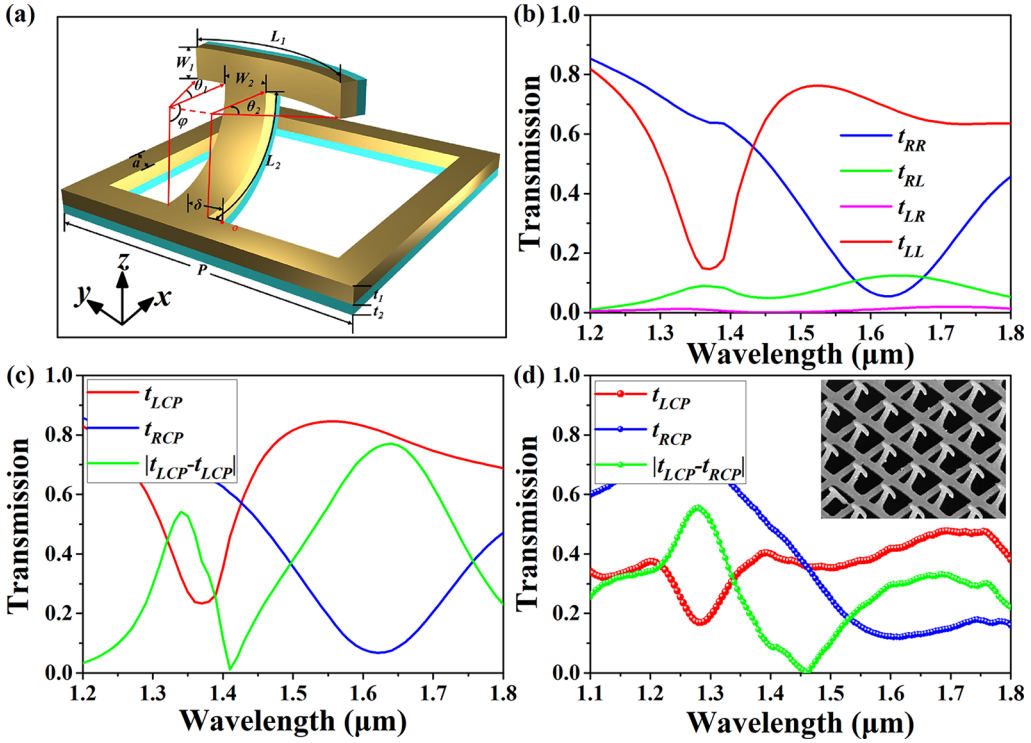

Figure 5. (a) Schematic of the structural parameters of the T-shaped curled metasurface with structure parameters: L_1 = 600 nm, L_2 = 550 nm, W_1 = 100 nm, W_2 = 150 nm, δ = 130 nm, a = 100 nm, t_1 = 50 nm, t_2 = 30 nm, P = 1000 nm, ϕ = 90°, θ_1 = 16.3°, and θ_2 = 52.8°, while δ is the distance between the upright rod and the central axis. (b) The squared moduli of the **T** matrix coefficients of the designed T-shaped curled metasurface. (c) Simulated and (d) measured transmission spectra and the absolute value of the transmission difference for the T-shaped curled metasurface under LCP and RCP illuminations. Inset: SEM image of the fabricated T-shaped curled metasurface.

further validated by the electric field distribution within the nanostructure. As shown in Figure 3g,h, the interaction between the Ent-A and LCP wave is much stronger than that between the Ent-A and RCP wave since the electric field on the surface of the nanostructures is significantly enhanced. The results in Figure 3c−h also validate that the L-shaped curled nanostructures play a key role in the spin-selective interaction between the proposed metasurfaces and the LCP (or RCP) wave. Thus, we further analyzed the influence of the structural parameters (L_1, L_2, θ, and ϕ) on the chiral optical response of the Ent-A in the Supporting Information, Figure S3. Results indicates that the resonant wavelength is directly related to the structural parameters L_1 and L_2. The variation of the curled angle ϕ will obviously change the strength of the chiral optical response. The relationship between the structural parameters and the chiral optical response of the Ent-A further validates that the L-shaped curled nanostructure dominates the chiral optical response of the Ent-A.

The giant chiral optical response in the Ent-A is further validated by experimental measurement with a custom-built optical setting, as shown in Figure 4a. The simulated and measured transmission spectra under LCP and RCP illuminations and the absolute value of the corresponding calculated transmission difference are shown in Figure 4b and c, respectively. Transmission difference with value over 60% can be observed in experiment at the wavelength of 1.5 μm, which is in good agreement with the simulated result, validating the spin-selective transmission in the designed L-shaped curled metasurfaces. Considering that a reflective objective with 0.2 numerical aperture was used in the experiment for light focusing, the incident angle is below to 12°. Within this range of incidence angles, we proved that the measured results are mainly due to the intrinsic chirality by quantitative analysis in Supporting Information, Figure S4. Due to the fabrication tolerances, the blue shift of the resonant peak can be ascribed to the minute difference in structural parameters between the designed and fabricated metasurfaces. The simulated and measured transmission difference in the proposed L-shaped curled metasurfaces is over 75% and 60%, respectively, which is unprecedented for most planar structures and comparable to or exceeding the chiral metamaterials with complex three-dimensional structures.[16,36−38]

It is worth mentioning that the curled metasurfaces fabricated by FIB-induced bending technology provide an effective approach for the realization of the intrinsic chirality. In general, for the design of the curled metasurface with intrinsic chirality, the breaking of the mirror symmetry of the whole structure is necessary while the structural configuration of the curled nanostructure can be further adjusted to manipulate the chiral optical response. Therefore, the curled metasurfaces based on other curled nanostructures can also be used to realize various chiral optical responses. We further designed and fabricated a T-shaped curled metasurface, as shown in Figure 5a. The structural mirror symmetry is broken when δ is not equal to zero (Supporting Information, Figure S5). Figure 5b shows the squared moduli of the **T** matrix coefficients of the designed T-shaped curled metasurface. The T-shaped curled metasurface shows opposite intrinsic chiral optical responses in two adjacent wavebands, presenting the spin-selective transmission of RCP and LCP waves at the wavelengths of 1.36 and 1.64 μm, respectively. The chirality of the T- shaped curled metasurface is also mainly attributed to

https://dx.doi.org/10.1021/acsphotonics.0c01230
ACS Photonics 2020, 7, 3415−3422

the spin-selective excitations of the electric dipole and the electric quadrupole (Supporting Information, Figures S6−S8). The simulated and measured transmission spectra for T-shaped curled metasurface under LCP and RCP illuminations and the absolute value of the corresponding calculated transmission difference are shown in Figure 5c and d, respectively. The simulated transmission differences are over 50% and 70% at the wavelength of 1.36 and 1.64 μm respectively, which are in reasonable agreement with the measured results. The noticeable deviation between the simulated and experimental results at the long wavelength is mainly attributed to the structural difference of the short arm of the T-shaped structures between the designed and fabricated metasurfaces.

In conclusion, we theoretically and experimentally demonstrated the use of curled metasurfaces for the implementation of the giant intrinsic chiral optical response. By utilizing the FIB-induced bending technology, the 3D curled nanostructures can be assembled from planar structure on nanoscale, which provide an effective approach for the breaking of structural mirror symmetry, offering a new alternative for the realization of giant chirality. The L-shaped and T-shaped curled metasurfaces were designed and fabricated to verify the giant chiral optical response in the curled metasurfaces. For the L-shaped curled metasurfaces, the spin-selective transmission with over 60% efficiency can be realized in the experiment at the wavelength of 1.5 μm, while the T-shaped curled metasurface shows opposite chiral optical responses at two adjacent wavebands. The curled metasurfaces provide a new and versatile strategy for the realization of giant intrinsic chirality, which shows a great potential for practical application in spin optics, quantum optics, and chiral sensing.

METHODS

Sample Fabrication. The fabrication process of curled metasurfaces with FIB-induced bending technology contains two parts: (1) planar pattern preparation: a SiN_x window with 20 nm thickness was purchased as substrate (Ilabilab Company), and the area of the windows was 100 × 100 μm^2. First, the SiN_x window was cleaned under an oxygen plasma atmosphere by RIE for 10 s, and the pressure was maintained at 100 mTorr with 100 sccm O_2 flow. Then, PMMA (495 A5) was spin-coated on the windows, and 200 nm thick PMMA film was obtained after 180 °C bake. The PMMA was patterned by electron beam lithography (EBL) and then RIE process, in which the etching duration of RIE process was 2 min under the power of 200 W, and the processing chamber maintained a 55 mTorr pressure with the gas flow of 5 sccm O_2 and 50 sccm CHF_3. After that, the residual PMMA was then removed by RIE. Finally, Au with a thickness of 50 nm was deposited by magnetron sputtering to obtain patterned Au/SiN_x bilayer on the window. (2) FIB-induced bending: The patterned bilayer membrane was placed into the chamber of a FIB/SEM system (Helios 600, FEI) with Ga ion source. The 2D planar patterns were bended to a curled structure by the ion irradiation process with area scanning, where the ion energies and ion beam current densities equal to 30 keV and 0.23 nA for 90 s, respectively. The irradiation area is more than 100 × 100 μm^2, which can achieve global irradiation. The metasurface with 90° bending angle was finally obtained. All the processes operated at the room temperature. It is worth mentioning that, according to our previous work, the content of Ga in the ion-irradiated bilayer film is pretty low compared with other elements, which can be negligible for the optical response of the fabricated samples.[43] The curvature (curled angle ϕ) is not depend on the structural configuration of the curled nanostructure, but the ion doses and ion energy. More specifically, the curvature is almost linearly proportional to the ion doses and ion energy, which can be precisely controlled in the process of irradiation. This feature ensured that our proposed curled metasurfaces are manufacturable and reproducible. More details about the FIB-induced bending technology can be found in ref 43.

Numerical Simulations. We implement 3D full-wave simulations with finite element method (COMSOL Multiphysics) to optimize the structural parameters and analyze the characterizations of the designed curled metasurfaces. In the simulation, the permittivity of SiN_x was taken as 3.8. The permittivity of gold was described by interpolated experimental values.[44] Periodic boundary conditions were imposed in the x- and y-directions to characterize the periodic structure, and the scattering boundary condition was set for wave illumination while the excitation source was either a left- or right-handed circularly polarized plane wave.

Experimental Measurement. The experiments were carried out through the use of a custom-built optical setting, as shown in Figure 4a. White light from a bromine tungsten lamp (BTL) was used as the light source. A linear polarizer (LP) and a quarter-wave plate (QWP) were used to control the polarization state of the incident light. In the experimental process, the spot size of the incident light was adjusted by utilizing a 4f-system composed of two lenses and an aperture to fit the size of the samples. The aperture was set near the focus of the 4f-system. A reflective objective (RO1) was used to focus the light on the sample. The transmission light through the sample was collected by using another reflective objective (RO2). Then the collected light passed through a prism and collected by an optical spectrum analyzer (OSA) via a fiber coupler and a CCD camera. All optical elements, including the microscope objective, lens, polarizers and detector, were operated in the broadband range.

ASSOCIATED CONTENT

Supporting Information

The Supporting Information is available free of charge at https://pubs.acs.org/doi/10.1021/acsphotonics.0c01230.

Analysis of the wide-angle optical response of the L-shaped curled metasurface, multipolar decomposition of the scattering spectra of the L-shaped curled metasurface, influence of the structural parameter variation on the chiral optical response of the L-shaped curled metasurface, a further analysis of the experimental results, influence of the structural parameter variation on the chiral optical response of the T-shaped curled metasurface, analysis of the intrinsic chirality in the T-shaped curled metasurface, and Figures S1−S8 (PDF)

AUTHOR INFORMATION

Corresponding Authors

Hua Cheng − *The Key Laboratory of Weak Light Nonlinear Photonics, Ministry of Education, School of Physics and TEDA Institute of Applied Physics, Nankai University, Tianjin 300071, China*; Email: hcheng@nankai.edu.cn

Shuqi Chen − *The Key Laboratory of Weak Light Nonlinear Photonics, Ministry of Education, School of Physics and*

https://dx.doi.org/10.1021/acsphotonics.0c01230
ACS Photonics 2020, 7, 3415−3422

TEDA Institute of Applied Physics, Nankai University, Tianjin 300071, China; The Collaborative Innovation Center of Extreme Optics, Shanxi University, Taiyuan, Shanxi 030006, China; Collaborative Innovation Center of Light Manipulations and Applications, Shandong Normal University, Jinan 250358, China; orcid.org/0000-0002-7898-4148; Email: schen@nankai.edu.cn

Authors

Chao Wang − *The Key Laboratory of Weak Light Nonlinear Photonics, Ministry of Education, School of Physics and TEDA Institute of Applied Physics, Nankai University, Tianjin 300071, China*

Zhancheng Li − *The Key Laboratory of Weak Light Nonlinear Photonics, Ministry of Education, School of Physics and TEDA Institute of Applied Physics, Nankai University, Tianjin 300071, China*

Ruhao Pan − *Beijing National Laboratory for Condensed Matter Physics, Institute of Physics, Chinese Academy of Sciences, Beijing 100190, China;* orcid.org/0000-0002-5573-2992

Wenwei Liu − *The Key Laboratory of Weak Light Nonlinear Photonics, Ministry of Education, School of Physics and TEDA Institute of Applied Physics, Nankai University, Tianjin 300071, China*

Junjie Li − *Beijing National Laboratory for Condensed Matter Physics, Institute of Physics, Chinese Academy of Sciences, Beijing 100190, China;* orcid.org/0000-0002-1508-9891

Wenyuan Zhou − *The Key Laboratory of Weak Light Nonlinear Photonics, Ministry of Education, School of Physics and TEDA Institute of Applied Physics, Nankai University, Tianjin 300071, China*

Jianguo Tian − *The Key Laboratory of Weak Light Nonlinear Photonics, Ministry of Education, School of Physics and TEDA Institute of Applied Physics, Nankai University, Tianjin 300071, China*

Complete contact information is available at: https://pubs.acs.org/10.1021/acsphotonics.0c01230

Author Contributions

‡C.W. and Z.L. contributed equally to this work. S.C. supervised the project. C.W. and W.L. carried out the design and simulation of the metasurfaces. R.P. fabricated the samples. Z.L., J.L., and H.C. performed the measurement. Z.L., W.L., H.C., and S.C. analyzed the data. Z.L., C.W., S.C., W.Z., and J.T. wrote the manuscript. All authors contributed to the discussion of the manuscript.

Notes

The authors declare no competing financial interest.

■ ACKNOWLEDGMENTS

This work was supported by the National Key Research and Development Program of China (2016YFA0301102 and 2017YFA0303800), the National Natural Science Fund for Distinguished Young Scholar (11925403), the National Natural Science Foundation of China (11974193, 11904181, 11904183, 91856101, and 11774186), Natural Science Foundation of Tianjin for Distinguished Young Scientists (18JCJQJC45700), the National Postdoctoral Program for Innovative Talents (BX20180148), and the China Postdoctoral Science Foundation (2018M640224 and 2018M640229).

■ REFERENCES

(1) Hentschel, M.; Schäferling, M.; Duan, X.; Giessen, H.; Liu, N. Chiral plasmonics. *Sci. Adv.* **2017**, *3*, No. e1602735.
(2) Sharma, V.; Crne, M.; Park, J. O.; Srinivasarao, M. Structural origin of circularly polarized iridescence in jeweled beetles. *Science* **2009**, *325*, 449−451.
(3) Schäferling, M. Chiral Nanophotonics. *Springer Ser. Opt. Sci.* **2017**, *205*, 159.
(4) Wang, Z.; Cheng, F.; Winsor, T.; Liu, Y. Optical chiral metamaterials: a review of the fundamentals, fabrication methods and applications. *Nanotechnology* **2016**, *27*, 412001.
(5) Collins, J. T.; Kuppe, C.; Hooper, D. C.; Sibilia, C.; Centini, M.; Valev, V. K. Chirality and chiroptical effects in metal nanostructures: fundamentals and current trends. *Adv. Opt. Mater.* **2017**, *5*, 1700182.
(6) Ma, X.; Pu, M.; Li, X.; Guo, Y.; Gao, P.; Luo, X. Meta-chirality: Fundamentals, construction and applications. *Nanomaterials* **2017**, *7*, 116.
(7) Luo, Y.; Chi, C.; Jiang, M.; Li, R.; Zu, S.; Li, Y.; Fang, Z. Plasmonic chiral nanostructures: chiroptical effects and applications. *Adv. Opt. Mater.* **2017**, *5*, 1700040.
(8) Chen, S.; Li, Z.; Liu, W.; Cheng, H.; Tian, J. From Single-Dimensional to Multidimensional Manipulation of Optical Waves with Metasurfaces. *Adv. Mater.* **2019**, *31*, 1802458.
(9) Zhao, Y.; Belkin, M. A.; Alù, A. Twisted optical metamaterials for planarized ultrathin broadband circular polarizers. *Nat. Commun.* **2012**, *3*, 870.
(10) Hentschel, M.; Schäferling, M.; Weiss, T.; Liu, N.; Giessen, H. Three-dimensional chiral plasmonic oligomers. *Nano Lett.* **2012**, *12*, 2542−2547.
(11) Cui, Y.; Kang, L.; Lan, S.; Rodrigues, S.; Cai, W. Giant chiral optical response from a twisted-arc metamaterial. *Nano Lett.* **2014**, *14*, 1021−1025.
(12) Decker, M.; Zhao, R.; Soukoulis, C. M.; Linden, S.; Wegener, M. Twisted split-ring-resonator photonic metamaterial with huge optical activity. *Opt. Lett.* **2010**, *35*, 1593−1595.
(13) Knipper, R.; Mayerhöfer, T. G.; Kopecky, V., Jr.; Huebner, U.; Popp, J. Observation of giant infrared circular dichroism in plasmonic 2D-metamaterial arrays. *ACS Photonics* **2018**, *5*, 1176−1180.
(14) Fasold, S.; Linß, S.; Kawde, T.; Falkner, M.; Decker, M.; Pertsch, T.; Staude, I. Disorder-enabled pure chirality in bilayer plasmonic metasurfaces. *ACS Photonics* **2018**, *5*, 1773−1778.
(15) Wang, Z.; Jia, H.; Yao, K.; Cai, W.; Chen, H.; Liu, Y. Circular dichroism metamirrors with near-perfect extinction. *ACS Photonics* **2016**, *3*, 2096−2101.
(16) Zhu, A. Y.; Chen, W. T.; Zaidi, A.; Huang, Y.-W.; Khorasaninejad, M.; Sanjeev, V.; Qiu, C.-W.; Capasso, F. Giant intrinsic chiro-optical activity in planar dielectric nanostructures. *Light: Sci. Appl.* **2018**, *7*, 17158.
(17) Chen, S.; Reineke, B.; Li, G.; Zentgraf, T.; Zhang, S. Strong Nonlinear Optical Activity Induced by Lattice Surface Modes on Plasmonic Metasurface. *Nano Lett.* **2019**, *19*, 6278−6283.
(18) Rajaei, M.; Zeng, J.; Albooyeh, M.; Kamandi, M.; Hanifeh, M.; Capolino, F.; Wickramasinghe, H. K. Giant circular dichroism at visible frequencies enabled by plasmonic ramp-shaped nanostructures. *ACS Photonics* **2019**, *6*, 924−931.
(19) Hu, Z.; Meng, D.; Lin, F.; Zhu, X.; Fang, Z.; Wu, X. Plasmonic Circular Dichroism of Gold Nanoparticle Based Nanostructures. *Adv. Opt. Mater.* **2019**, *7*, 1801590.
(20) Ma, D.; Li, Z.; Zhang, Y.; Liu, W.; Cheng, H.; Chen, S.; Tian, J. Giant spin-selective asymmetric transmission in multipolar-modulated metasurfaces. *Opt. Lett.* **2019**, *44*, 3805−3808.
(21) Basiri, A.; Chen, X.; Bai, J.; Amrollahi, P.; Carpenter, J.; Holman, Z.; Wang, C.; Yao, Y. Nature-inspired chiral metasurfaces for circular polarization detection and full-Stokes polarimetric measurements. *Light: Sci. Appl.* **2019**, *8*, 78.
(22) Wang, Q.; Plum, E.; Yang, Q.; Zhang, X.; Xu, Q.; Xu, Y.; Han, J.; Zhang, W. Reflective chiral meta-holography: multiplexing holograms for circularly polarized waves. *Light: Sci. Appl.* **2018**, *7*, 25.

(23) Li, W.; Coppens, Z. J.; Besteiro, L. V.; Wang, W.; Govorov, A. O.; Valentine, J. Circularly polarized light detection with hot electrons in chiral plasmonic metamaterials. *Nat. Commun.* **2015**, *6*, 8379.
(24) Jing, L.; Wang, Z.; Yang, Y.; Zheng, B.; Liu, Y.; Chen, H. Chiral metamirrors for broadband spin-selective absorption. *Appl. Phys. Lett.* **2017**, *110*, 231103.
(25) Plum, E.; Zheludev, N. I. Chiral mirrors. *Appl. Phys. Lett.* **2015**, *106*, 221901.
(26) Kang, L.; Rodrigues, S. P.; Taghinejad, M.; Lan, S.; Lee, K.-T.; Liu, Y.; Werner, D. H.; Urbas, A.; Cai, W. Preserving spin states upon reflection: linear and nonlinear responses of a chiral meta-mirror. *Nano Lett.* **2017**, *17*, 7102−7109.
(27) Chen, Y.; Gao, J.; Yang, X. Chiral Metamaterials of Plasmonic Slanted Nanoapertures with Symmetry Breaking. *Nano Lett.* **2018**, *18*, 520−527.
(28) Chen, Y.; Yang, X.; Gao, J. 3D Janus plasmonic helical nanoapertures for polarization-encrypted data storage. *Light: Sci. Appl.* **2019**, *8*, 45.
(29) Chen, Y.; Yang, X.; Gao, J. Spin-controlled wavefront shaping with plasmonic chiral geometric metasurfaces. *Light: Sci. Appl.* **2018**, *7*, 84.
(30) Hendry, E.; Carpy, T.; Johnston, J.; Popland, M.; Mikhaylovskiy, R. V.; Lapthorn, A. J.; Kelly, S. M.; Barron, L. D.; Gadegaard, N.; Kadodwala, M. Ultrasensitive detection and characterization of biomolecules using superchiral fields. *Nat. Nanotechnol.* **2010**, *5*, 783−787.
(31) Schaferling, M.; Dregely, D.; Hentschel, M.; Giessen, H. Tailoring Enhanced Optical Chirality: Design Principles for Chiral Plasmonic Nanostructures. *Phys. Rev. X* **2012**, *2*, 031010.
(32) Ho, C.-S.; Garcia-Etxarri, A.; Zhao, Y.; Dionne, J. Enhancing Enantioselective Absorption Using Dielectric Nanospheres. *ACS Photonics* **2017**, *4*, 197−203.
(33) Yao, K.; Liu, Y. Enhancing circular dichroism by chiral hotspots in silicon nanocube dimers. *Nanoscale* **2018**, *10*, 8779−8786.
(34) Yao, K.; Zheng, Y. Near-Ultraviolet Dielectric Metasurfaces: from Surface-Enhanced Circular Dichroism Spectroscopy to Polarization-Preserving Mirrors. *J. Phys. Chem. C* **2019**, *123*, 11814−11822.
(35) Gansel, J. K.; Thiel, M.; Rill, M. S.; Decker, M.; Bade, K.; Saile, V.; von Freymann, G.; Linden, S.; Wegener, M. Gold helix photonic metamaterial as broadband circular polarizer. *Science* **2009**, *325*, 1513−1515.
(36) Sakellari, I.; Yin, X.; Nesterov, M. L.; Terzaki, K.; Xomalis, A.; Farsari, M. 3D chiral plasmonic metamaterials fabricated by direct laser writing: the twisted omega particle. *Adv. Opt. Mater.* **2017**, *5*, 1700200.
(37) Li, Z.; Liu, W.; Cheng, H.; Chen, S.; Tian, J. Spin-selective transmission and devisable chirality in two-layer metasurfaces. *Sci. Rep.* **2017**, *7*, 8204.
(38) Duan, X.; Yue, S.; Liu, N. Understanding complex chiral plasmonics. *Nanoscale* **2015**, *7*, 17237−17243.
(39) Liu, Z.; Du, S.; Cui, A.; Li, Z.; Fan, Y.; Chen, S.; Li, W.; Li, J.; Gu, C. High-Quality-Factor Mid-Infrared Toroidal Excitation in Folded 3D Metamaterials. *Adv. Mater.* **2017**, *29*, 1606298.
(40) Yang, S.; Liu, Z.; Hu, S.; Jin, A.-Z.; Yang, H.; Zhang, S.; Li, J.; Gu, C. Spin-selective transmission in chiral folded metasurfaces. *Nano Lett.* **2019**, *19*, 3432−3439.
(41) Cui, A.; Liu, Z.; Li, J.; Shen, T. H.; Xia, X.; Li, Z.; Gong, Z.; Li, H.; Wang, B.; Li, J.; Yang, H.; Li, W.; Gu, C. Directly patterned substrate-free plasmonic "nanograter" structures with unusual Fano resonances. *Light: Sci. Appl.* **2015**, *4*, No. e308.
(42) Wu, P. C.; Liao, C. Y.; Savinov, V.; Chung, T. L.; Chen, W. T.; Huang, Y.-W.; Wu, P. R.; Chen, Y.-H.; Liu, A.-Q.; Zheludev, N. I.; Tsai, D. P. Optical anapole metamaterial. *ACS Nano* **2018**, *12*, 1920−1927.
(43) Pan, R.; Li, Z.; Liu, Z.; Zhu, W.; Zhu, L.; Li, Y.; Chen, S.; Gu, C.; Li, J. Rapid Bending Origami in Micro/Nanoscale toward a Versatile 3D Metasurface. *Laser Photonics Rev.* **2020**, *14*, 1900179.
(44) Palik, E. D. *Handbook of Optical Constants of Solids*; Academics Press: NY, 1998.

https://dx.doi.org/10.1021/acsphotonics.0c01230
ACS Photonics 2020, 7, 3415−3422